

# Large-area topography analysis and near-field Raman spectroscopy using bent fibre probes

J. PRIKULIS\*, K. V. G. K. MURTY\*, H. OLIN† & M. KÄLL\*

Departments of \*Applied Physics and †Experimental Physics, Chalmers University of Technology, SE-412 96 Göteborg, Sweden

**Key words.** Colloidal silver nanoparticles, near-field optics, surface-enhanced Raman spectroscopy.

## Summary

We present a method for combined far-field Raman imaging, topography analysis and near-field spectroscopy. Surface-enhanced Raman spectra of Rhodamine 6G (R6G) deposited on silver nanoparticles were recorded using a bent fibre aperture-type near-field scanning optical microscope (NSOM) operated in illumination mode. Special measures were taken to enable optical normal-force detection for control of the tip–sample distance. Comparisons between far-field Raman images of R6G-covered Ag particle aggregates with topographic images recorded using atomic force microscopy (AFM) indicate saturation effects due to resonance excitation.

## Introduction

Near-field scanning optical microscopy (NSOM) makes it possible to analyse optical properties with a spatial resolution better than the Abbe limit, and to obtain combined spectroscopic and topographic information of complex surfaces (Betzig & Trautman, 1992; Hecht *et al.*, 2000). NSOM techniques have been used successfully for fluorescence spectroscopy, even of single dye molecules with sufficiently high fluorescence yield (Trautman *et al.*, 1994). There is now growing interest in using NSOM for localized Raman spectroscopy (Jahncke *et al.*, 1995; Emory & Nie, 1997; Webster *et al.*, 1998; Stöckle *et al.*, 2000; Zenobi & Deckert, 2000). However, the poor Raman cross-section (typically  $10^{-30}$  cm<sup>2</sup> for a nonresonant molecule), limited light throughput of the subwavelength metallic aperture ( $\approx 10^{-6}$  for a 50-nm aperture probe) and the limited laser power that the fibre can withstand, makes the measurements very time-consuming.

The reason for the light intensity losses is basically the cut-off frequency of the waveguide formed by the tapered fibre. Part of the light is reflected and part is dissipated as heat. The

intensity loss in an aperture of diameter  $d$  grows as  $d^{-4}$ , thus for smaller apertures the risk of thermal damage of the tip limits the power that can be coupled to the fibre (La Rosa *et al.*, 1995). The development of practical, usable aperture probes has stopped at diameters around 50 nm. The penetration depth of the light in the metal coating is another hindrance for the fabrication of smaller apertures.

In order to acquire near-field Raman spectral information, despite the above difficulties, one may artificially increase the effective molecular Raman cross-section using surface-enhanced Raman scattering (SERS). A particularly large surface enhancement is achieved when certain molecules are adsorbed at nanostructured noble metal surfaces, e.g. in the form of colloidal particles. The higher effective cross-sections achieved by SERS have been used to detect molecules at very low concentrations, even at the single molecule level (Nie & Emory, 1997; Kneipp *et al.*, 1999; Xu *et al.*, 1999).

In this study, far-field Raman images and near-field Raman spectra of the chromophore Rhodamine 6G (R6G) adsorbed on silver particles are presented and compared with topographical images of the particles. Near-field Raman experiments on similar samples were performed by Emory & Nie (1997) and Stöckle *et al.* (2000) using straight fibre probes and shear-force distance regulation. Normal-force distance regulation, as used here, reduces the risk of probe damage and simplifies sample scanning over large areas.

## Experimental methods and materials

A modified commercial NSOM head (Nanonics NSOM-100) was central to the experimental setup (Fig. 1). The design of the system allowed for both near- and far-field Raman measurements, as well as imaging of the same area using an atomic force microscope (AFM) without removing the sample. In addition, the microscope objective could be placed below and above (not shown) the sample, thus allowing near-field experiments in transmission and reflection mode. All measurements in this report were carried out in the transmission mode.

Correspondence to: J. Prikulis. Tel. +46 31 772 3300; fax: +46 31 772 2090; e-mail: prikulis@fy.chalmers.se

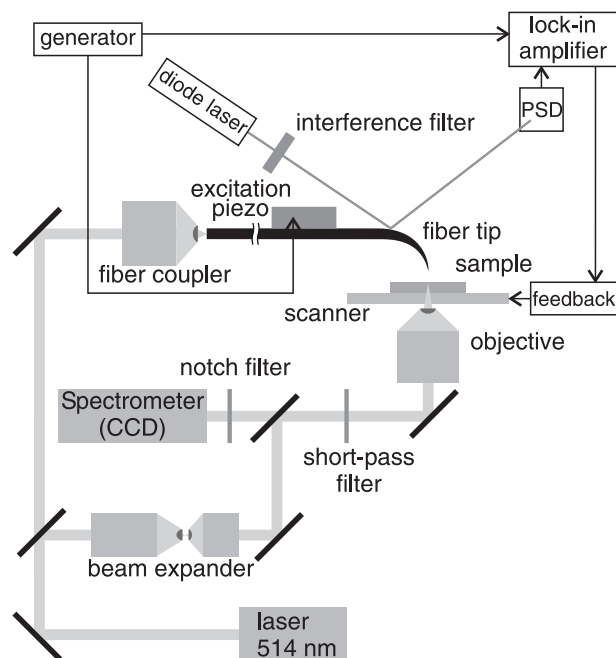


Fig. 1. Schematic view of the experimental setup.

#### Near-field measurements

We used commercial Cr/Al-coated fibre probes (Nanonics) with apertures down to 50 nm to illuminate the sample. A Newport fibre-coupler with a  $\times 10$ , NA 0.21, objective was used to couple the 514 nm laser line from an Ar<sup>+</sup> laser to the fibre. The measured input power before the coupler was 25 mW. Scattered light was collected in the far-field using a long-working-distance objective (Nikon  $\times 40$ , NA 0.55) and directed to the spectrometer (Renishaw Ramascope RM 2000). A holographic notch-filter (Kaiser) prevents the excitation light from reaching the detector.

#### AFM imaging

In aperture-type NSOM applications, the shear-force method is widely used for tip-sample distance control, as the well-established straight fibre probes can be used (Durkan & Shvets, 1996). Shear-force distance probes control requires flat samples for scanning, and because the damping depends on the sample material, it does not guarantee correct topography for samples consisting of different materials (Durkan & Shvets, 1996). Not only does the shape of the tip influence the lateral resolution, but so too does the dithering amplitude of the tip. A less restricted distance regulation is based on normal force sensing between a bent fibre tip and the sample surface (Wolf *et al.* 1999). Increasing the input power can compensate for the lower throughput of the bent probes without thermal damage, as the extra  $\approx 30\%$  intensity loss compared with straight probes occurs in the kink of the waveguide and not in the

probe apex. The bent fibre probe is excited normally to the sample surface (Stephenson & Welland 1996) at its resonance frequency, which for Nanonics NSOM-AFM probes lies within the 100–200 kHz range. An optical method is used to detect the dithering amplitude: light from a laser diode is reflected by the metallized surface of the tip and directed to a position sensitive detector (PSD), after which the detected signal is lock-in amplified and used as input to the feedback circuit. The oscillations of the tip are damped as the distance to the sample decreases. Ninety per cent of the free oscillation amplitude was used as the set-point for the AFM feedback. The vertical movement of the tip influences the illumination of the sample. For the near-field conditions to be met, the distance between the aperture and the sample should be much less than the wavelength of the incident radiation. We assume that, because the illuminated area is larger when the tip is further away from the sample, and the light collection time is much larger than the period of tip oscillation, the effective aperture is slightly larger than the actual aperture. The probe excitation voltage was kept at 50 mV peak-to-peak. From the corresponding force curve we estimate the tip oscillation amplitude to be  $< 100$  nm.

The side-band intensity of the 671 nm diode laser radiation, used for distance regulation, is high compared with the extremely low intensity of the Raman-scattered light. We therefore added an interference filter with the same central wavelength directly after the diode laser. A band-pass filter (400–590 nm) positioned after the main objective lens then eliminates the central peak.

We used a home-built digital AFM controller and software. Scanning was carried out at a constant speed of  $\approx 2 \mu\text{m s}^{-1}$ . For smaller scan areas this speed was reduced to maintain the scan frequency to  $< 1 \text{ line s}^{-1}$ , because of the somewhat low resonance frequency of the scanner.

#### Raman imaging

A Renishaw Ramascope (RM 2000) equipped with a Leica microscope (DMLM series) and a motorized stage were used to record the Raman spectra and global images. Scattered light was detected by a charge coupled device (CCD) cooled to  $-70^\circ\text{C}$  by a Peltier cooling system. The spectrometer uses a grating for acquisition of the line scan spectra and angle-tuned bandpass optical filters for global images. Global Raman images were collected by positioning the angle-tuned band-pass filters at a desired wavenumber of the SERS spectrum. A larger area ( $\approx 20 \mu\text{m}$  in diameter) of the sample was illuminated by a defocused laser spot. The typical accumulation times for far-field Raman spectra and global images are 10 and 180 s, respectively.

#### Sample preparation

Analytical reagent grade R6G, sodium citrate, sodium chloride and 2-aminopropyltrimethoxysilane (APTMS) were acquired

from Sigma-Aldrich. All solutions were made by using deionized water (Milli-Q plus). The silver sol was prepared using a modified citrate reduction protocol, following Lee & Meisel (1982). The average size of the silver particles was  $\approx 90$  nm. The silver sol was stable for months without aggregation and was tested by its characteristic extinction spectrum.

The sample solution used for the SERS spectra was prepared by mixing the sol initially with NaCl solution to activate it and then with R6G solution. The final concentration of NaCl and R6G in the solution was maintained at 0.25 mM and  $10^{-7}$  M, respectively.

SERS substrates were prepared by depositing a required amount of the above solution on polymer-coated glass surfaces, which were prepared by coating self-assembled monolayers of APTMS onto glass surfaces (Freeman *et al.*, 1995). For a uniform coverage of the surface with the silver particles the above solution was kept on the surface for 45 s. By varying this deposition time, one can alter the density of the surface coverage by the silver particles.

## Results

Fig. 2 shows topographical mapping by AFM and global Raman imaging of R6G-coated silver particles on APTMS-covered glass surfaces. A  $16 \times 16 \mu\text{m}$  area was selected for the above measurements. The AFM image (Fig. 2a) shows silver aggregates with lateral dimensions ranging from 400 nm to 1  $\mu\text{m}$ . From the studies on the sol it was found that the average size of the colloid was  $\approx 90$  nm. Differences in the lateral dimensions suggest that these structures are 'flat' aggregates composed of several silver particles. The global Raman image of the same area (Fig. 2b) was acquired by detecting the  $1650 \text{ cm}^{-1}$  Raman peak, which corresponds to the fundamental vibration of the aromatic carbon-carbon stretch in R6G. Note that we used a comparatively high concentration of R6G in order to acquire a uniform coverage on the silver particles. The R6G concentration during the sample preparation corresponds to  $\approx 1000$  molecules per single silver particle. It is observed that the silver sol aggregates at such concentrations of R6G, which accounts for the appearance of large aggregates on the glass surface. Comparison of the topographical image of the surface by AFM and the Raman image of the same area shows interesting differences. The presence of certain bright aggregates in the Raman image qualitatively agrees with the reported literature on SERS (Nie & Emory, 1997; Xu *et al.*, 1999) where it is observed that certain sites are more SERS active or 'hot' than others. By contrast, by plotting the Raman intensity vs. the volume of the particle aggregate in the AFM image (Fig. 3) we observe a monotonous dependence, although with considerable scatter. This is in contrast to SERS data acquired using low concentrations of R6G, reported by, for example, Nie & Emory (1997), where only a very small fraction of the investigated nanoparticles exhibited a measurable SERS intensity. Based on the latter results, one would

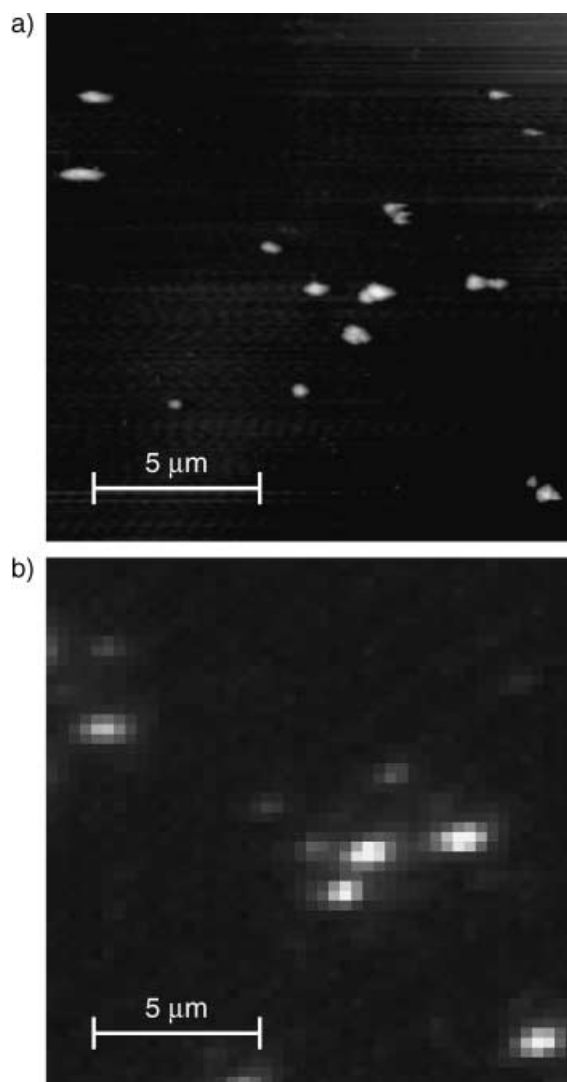


Fig. 2. Imaging of  $16 \times 16 \mu\text{m}$  area of R6G-covered Ag particles deposited on APTMS-coated glass. (a) AFM image with Z range 166 nm, (b) Raman image.

expect the intensity variation between different 'hot spots' to be several orders of magnitude, which was not observed in our study. In this context, it is important to note that the illumination wavelength, 514.5 nm, lies within the absorption band of R6G, i.e. the data should be treated as surface-enhanced resonance Raman scattering (SERRS). This indicates that the 'additive' nature of the Raman signal, i.e. that the Raman intensity scales with aggregate volume, is linked to a finite lifetime of the resonantly pumped nanoparticle/R6G excited states, which leads to saturation of the surface-enhanced signal even at moderate illumination intensities. For near-field spectroscopy (Fig. 4) the NSOM probe is positioned on the particle or aggregate in the focus of the collection objective. In contrast to the global Raman images, we were able to detect the SERS signal from a very small number (2 of  $\approx 100$ ) of particles

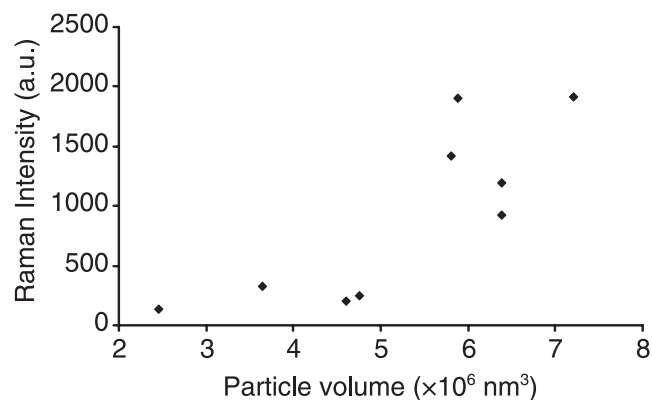


Fig. 3. Raman intensity vs. aggregate volume. The volume was estimated by integrating the height profile from the AFM image. Tip convolution effects increase the measured volume, i.e. the data points are shifted to the right.

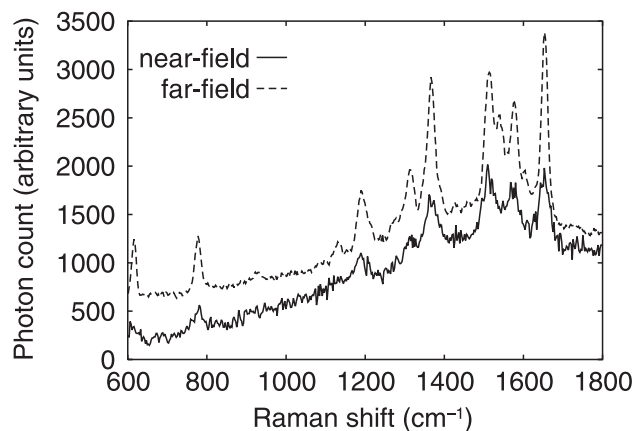


Fig. 4. Near- and far-field spectra of R6G deposited on a silver particle or particle aggregate.

or particle clusters. The near-field spectra show the same features as the far-field spectra, with almost the same line widths, and there are no indications of NSOM-induced gradient-field Raman effects (Ayars *et al.*, 2000). The long accumulation time ( $\approx 10$  min) needed to record a single near-field spectrum with a good signal-to-noise ratio, together with thermal drift, prevents acquisition of near-field Raman images, spectra were therefore measured on particles previously selected by AFM. A lateral resolution of 250 nm was estimated by recording intensity of elastically scattered light from Ag nanoparticles as a function of sample position. The geometry of the NSOM probes makes positioning of the aperture on the smaller particles ( $< 100$  nm diameter), for the accumulation of near-field spectra, difficult. A sharp extension in the metal coating of the tip may act as a 'mini-tip' (Fig. 5b) and give the largest contribution to the AFM image. Because the mini-tip does not coincide with the centre of the NSOM aperture, the particle may not be illuminated when

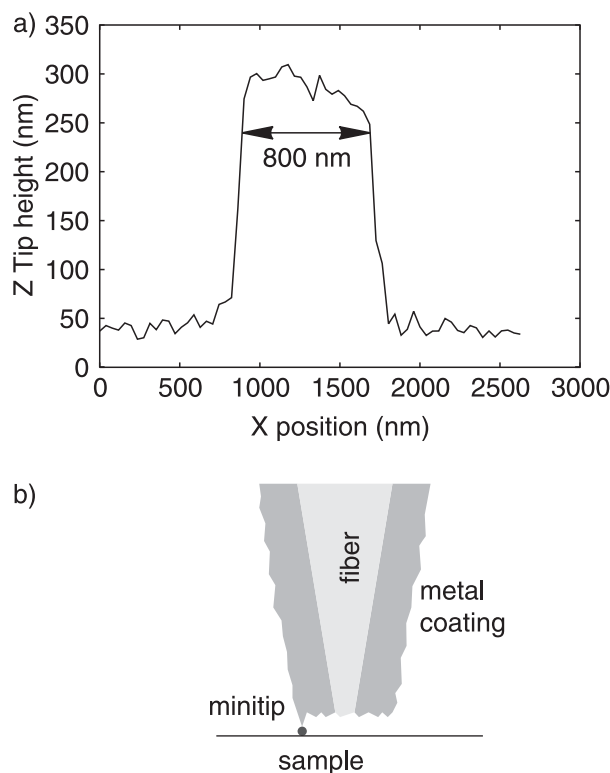


Fig. 5. Illustration of a tip artefact. (a) Measured cross-section of a NSOM-AFM probe (b) Aperture with a mini-tip.

AFM is used for positioning the tip at the particle. We have taken AFM images of a fresh 50 nm aperture tip using a tip characterization sample (TGT from NT-MDT). As can be seen in Fig. 5(a) the actual diameter of the tip is  $\approx 800$  nm. The difficulties associated with the displacement of the centre of the aperture with respect to the sharpest mini-tip would be reduced by individual characterization of each probe. This can be achieved, for example, by simultaneous AFM and elastic scattering NSOM imaging of small ( $< 50$  nm in diameter) Ag spheres.

## Conclusions

In conclusion, we have shown the possibility of using bent probes for near-field SERS experiments, despite reduced throughput and increased effective distance between the aperture and the sample. Normal-force distance regulation allows scanning of very large areas (side lengths 20–30  $\mu\text{m}$ ). The recorded near-field SERS spectra of R6G did not show significant differences from the far-field spectra. Combined AFM topography and wide-field Raman analysis of R6G-nanoparticle aggregates indicated saturation effects associated with resonance excitation.

## References

- Ayars, E.D., Hallen, H.D. & Jahncke, C.L. (2000) Electric field gradient effects in Raman spectroscopy. *Phys. Rev. Lett.* **85**, 4180–4183.

- Betzig, E. & Trautman, J.K. (1992) Near-field optics – microscopy, spectroscopy, and surface modification beyond the diffraction limit. *Science*, **257**, 189–195.
- Durkan, C. & Shvets, I.V. (1996) Investigation of the physical mechanisms of shear-force imaging. *J. Appl. Phys.* **80**, 5659–5664.
- Emory, S.R. & Nie, S.M. (1997) Near-field surface-enhanced Raman spectroscopy on single silver nanoparticles. *Anal. Chem.* **69**, 2631–2635.
- Freeman, R.G., Grabar, K.C., Allison, K.J. *et al.* (1995) Self-assembled metal colloid monolayers – an approach to sers substrates. *Science*, **267**, 1629–1632.
- Hecht, B., Sick, B., Wild, U.P. *et al.* (2000) Scanning near-field optical microscopy with aperture probes: fundamentals and applications. *J. Chem. Phys.* **112**, 7761–7774.
- Jahncke, C.L., Paesler, M.A. & Hallen, H.D. (1995) Raman imaging with near-field scanning optical microscopy. *Appl. Phys. Lett.* **67**, 2483–2485.
- Kneipp, K., Kneipp, H., Itzkan, I., Dasari, R.R. & Feld, M.S. (1999) Surface-enhanced non-linear Raman scattering at the single-molecule level. *Chem. Phys.* **247**, 155–162.
- La Rosa, A.H.L., Yakobson, B.I. & Hallen, H.D. (1995) Origins and effects of thermal-processes on near-field optical probes. *Appl. Phys. Lett.* **67**, 2597–2599.
- Lee, P.C. & Meisel, D. (1982) Adsorption and surface-enhanced Raman of dyes on silver and gold sols. *J. Phys. Chem.* **86**, 3391–3395.
- Nie, S.M. & Emory, S.R. (1997) Probing single molecules and single nanoparticles by surface enhanced Raman scattering. *Science*, **275**, 1102–1106.
- Stephenson, R.J. & Welland, M.E. (1996) Normal force distance regulation scheme for near-field optical microscopy. *Appl. Phys. Lett.* **68**, 1607–1609.
- Stöckle, R., Deckert, V., Fokas, C., Zeisel, D. & Zenobi, R. (2000) Sub-wavelength Raman spectroscopy on isolated silver islands. *Vib. Spectrosc.* **22**, 39–48.
- Trautman, J.K., Macklin, J.J., Brus, L.E. & Betzig, E. (1994) Near-field spectroscopy of single molecules at room-temperature. *Nature*, **369**, 40–42.
- Webster, S., Batchelder, D.N. & Smith, D.A. (1998) Submicron resolution measurement of stress in silicon by near-field Raman spectroscopy. *Appl. Phys. Lett.* **72**, 1478–1480.
- Wolf, J.F., Hillner, P.E., Bilewicz, R., Kölsch, P. & Rabe, J.P. (1999) Novel scanning near-field optical microscope (NSOM)/scanning confocal optical microscope based on normal force distance regulation and bent etched fiber tips. *Rev. Sci. Instr.* **70**, 2751–2757.
- Xu, H.X., Bjerneld, E.J., Käll, M. & Börjesson, L. (1999) Spectroscopy of single hemoglobin molecules by surface enhanced Raman scattering. *Phys. Rev. Lett.* **83**, 4357–4360.
- Zenobi, R. & Deckert, V. (2000) Scanning near-field optical microscopy and spectroscopy as a tool for chemical analysis. *Angew. Chem.-Int. Edit.* **39**, 1746–1756.